Quantum Circuit Execution as Unified Audiovisual Composition:
Full Quantum State Tomography Transduced into Virtual Reality Expression

Michael Rhoades, Ph.D.
IDIA Lab, Ball State University
mjrhoades@bsu.edu

Abstract

This paper documents the third phase of ongoing research and creative praxis, under the auspices of the Quantum Computational Creativity (QCC) endeavor, which is centered on quantum hardware execution, machine intelligence (MI) collaboration, and human creative agency. In Phase III, full quantum state tomography captures the pre-measurement states of eight qubits during composed circuit executions, measuring Bloch sphere coordinates across three complementary bases. These trajectories, which are records of quantum hardware behavior including entanglement correlations, decoherence, and wavefunction collapse, are transduced directly into time-based audio and visual material without intermediary interpretation.

Azimuth, elevation, and distance values derived from Bloch coordinates drive audio waveform generation and 8-channel 3D/360° Vector-Based Amplitude Panning (VBAP) and Ambisonics spatialization. Eight visual objects, each representing one qubit, are positioned and animated within stereoscopic 3D/360° environments, their motions, spatial localizations, and scalar proportions governed entirely by the same tomographic measurements. This shared data origin establishes a direct, mathematically precise, correspondence between the audio and visual components, which are accurate expressions of the quantum physical processes occurring during circuit execution.

Eight entanglement schemas, each producing a distinct quantum topology, yield eight audio/visual expressions assembled into a single coherent composition, *Dance of the Qubits,* ideally intended for virtual reality venues including head-mounted display cinemas and 3D/360° full immersion domes. This multi-modal creative expression of unified quantum-derived wavefunction transduction is poised as a significant breakthrough in QCC and forms a basis upon which further exploration will build. The aesthetics of the resultant composition are intended as a new frontier of creative expression.

1. Introduction

Quantum Computational Creativity (QCC) is an ongoing research and creative praxis program centered on the direct transduction of quantum hardware execution into novel artistic expression. Operating through a three-way symbiosis of quantum physical systems, machine intelligence (MI) collaboration, and human creative agency, QCC positions the quantum computer not as a computational tool applied to artistic ends, but as a generative participant whose physical

behavior constitutes the primary creative material. This paper presents the third phase of that program.

A foundational principle of QCC is the engagement with quantum computing in manners unavailable to classical computation. Quantum hardware execution produces phenomena such as entanglement correlations, decoherence, quantum noise, and wavefunction collapse that are not merely difficult to simulate classically but are physically distinct from anything classical systems can generate. Comparative experimentation conducted in earlier phases of this research confirmed that simulated quantum circuit execution, while useful for development and testing, does not carry the richness of results quantum hardware execution exhibits. This distinction is not incidental; it is the motivation for engaging with quantum computing as a creative medium.

Phase III extends the QCC methodology into new territory through the application of full quantum state tomography to eight composed entanglement circuit schemas executed on Quantum Inspire's Tuna-9 quantum processor. Where earlier phases employed quantum expectation values as the primary data source, Phase III reconstructs the complete Bloch sphere state of each qubit across three complementary measurement bases at each of 600 parameter steps per schema. The resulting trajectories encode entanglement correlations, decoherence signatures, and hardware noise as three-dimensional coordinate data and are transduced directly into both stereoscopic visual art and spatial audio composition without intermediary interpretation. Both the audio and visual material derive from identical quantum datasets, thus establishing mathematically precise correspondences between perceptual domains that are inherent rather than editorially constructed.

The eight entanglement schemas yield eight distinct audio/visual expressions, assembled into a unified composition titled *Dance of the Qubits,* intended for presentation in immersive virtual reality venues. The work represents a significant expansion of the QCC methodology from audio alone in earlier phases to a unified audio/visual medium here and introduces findings with direct implications for the design of future quantum circuits as compositional instruments.

This paper is organized as follows: Section 2 establishes the conceptual framework underlying the methodology. Section 3 describes the quantum state tomography pipeline. Sections 4 and 5 detail the visual and audio transduction pipelines respectively. Section 6 addresses the unification of audio and visual material into a single coherent composition and the production pipeline through which that unification is realized. Section 7 presents key findings and their implications. Section 8 offers conclusions and directions for future work.

2. Conceptual Framework

The methodology underlying this work rests on three interconnected principles: that quantum state tomography provides a richer and more complete data source than expectation values alone, that the Bloch sphere offers a geometrically natural bridge between quantum physical reality and perceptual space, and that a single quantum dataset can serve simultaneously as the generative

source for both audio and visual material thus producing correspondence that is mathematically inherent rather than editorially imposed.

Quantum state tomography reconstructs the full quantum state of a system from repeated measurements across multiple complementary bases. Rather than collapsing the qubit to a single binary outcome, tomography probes the qubit's state from three orthogonal perspectives; the X, Y, and Z bases. From these measurements the tomographic approach reconstructs the probability amplitudes that describe the qubit's position on the Bloch sphere at each determined interval throughout the circuit execution. This reconstruction yields three coordinates per qubit per parameter step, the Bloch x, y, and z values, which together encode the complete quantum state including superposition, entanglement correlations, decoherence, and hardware noise signatures. The Bloch radius, derived as $r = \sqrt{(x^2 + y^2 + z^2)}$, provides a measure of quantum purity, ranging from 1.0 for a pure state to 0.0 for a maximally mixed state.

The Bloch sphere is not merely a convenient visualization tool. It is a geometric representation of a qubit's quantum state space. Every point within or upon the surface of the Bloch sphere determines the quantum purity value and corresponds to a physically realizable qubit state. The trajectories traced by qubits through Bloch sphere space during circuit execution are therefore not abstractions or representations of quantum behavior; they are quantum behavior, expressed in a three-dimensional geometric form that is directly accessible to both audio and visual transduction. This is the conceptual foundation upon which the entire methodology rests.

The transduction principle holds that quantum-derived data should be translated into perceptual material directly, without intermediary interpretation. Where sonification imposes a representational layer between data and perception, transduction maintains a mathematically precise correspondence. With it the geometry of the quantum state space becomes the geometry of the perceptual space. In this project, this principle extends across two simultaneous perceptual domains. The same Bloch sphere coordinates that position visual objects in stereoscopic three-dimensional space also determine the spatial localization, temporal phrasing, and waveform characteristics of the audio material. Neither domain is primary; both are consequences of the same underlying quantum physical reality.

This shared origin has a profound implication for the resulting composition. The correspondence between audio and visual expression in *Dance of the Qubits* is not a synchronization achieved through post-production alignment, it is a mathematical identity. When the quantum system dwells in a high-purity state, both the visual filament and the audio event reflect that simultaneously, not because they have been aligned, but because the quantum data determined both. This represents a fundamental departure from conventional audiovisual composition, in which audio and visual are independent creative streams brought into relationship through editorial judgment.

Before proceeding, theoretical premises ascribed to by the QCC endeavor should be clearly stated to avoid any ambiguities that could exist within the following delineations. For it is considered fundamental that quantum particles exist within systems that constrain their behavior

at every scale, in every context, and within multifarious stratifications. Overly simplified examples would be that a particle in a molecule is constrained by its chemical environment and by the manner in which that environment interacts with other related systems. The behavior of a photon is affected by the gravitational geometry of nearby mass, a qubit in a biological system by thermal fluctuations and molecular geometry. Constraint is the natural condition of quantum reality in every configuration and at every level of interaction. Perhaps it is this lack of behavioral consistency that contributes to the challenge of comprehending quantum phenomena.

The quantum computer constrains qubits in very specific ways that are based upon humanistically imposed understandings. The environment of the quantum computer uniquely and specifically constrains the behavior of qubits in an extremely controlled system. This empowers experimentation in an unprecedented manner. Therefore, the circuit topologies, gate sequences, and the parameter sweeps of each schema explored in this project are compositional decisions that define the ranges of the qubit behaviors. The Bloch sphere trajectories we observe and transduce are quantum behavior as expressed through this particular nested system of interacting constraints, including the designed circuit architecture and the physical substrate of the transmon processor itself. From these perspectives, each reference to "quantum behavior" in this paper carries these qualifications implicitly.

3. Quantum State Tomography Pipeline

Quantum state tomography provides the data foundation for all subsequent audio and visual material in this work. Unlike expectation value measurement, which yields a single scalar per qubit per circuit execution, full state tomography reconstructs the complete quantum state of each qubit by probing it from three orthogonal measurement perspectives. The result is three-dimensional Bloch sphere coordinates that encode the full quantum behavior of the qubit at that moment. Pure states reside on the surface of the sphere; the decoherence and hardware noise inherent in real quantum execution produce mixed states whose reconstructed coordinates fall within it, which forms a physically accurate signature of quantum hardware that classical simulation cannot replicate. It is from these coordinates that all audio and visual material is derived.

3.1 Measurement Protocol

Each of the eight entanglement schemas is executed on Quantum Inspire's Tuna-9 processor (Last et al. 2020; Quantum Inspire 2025), a 9-qubit transmon system. For each schema, the circuit is executed across 600 discrete parameter steps, with each step measured across three complementary bases: Z, X, and Y. At each step and for each basis, 2048 shots are taken, which are repeated executions of the identical circuit from which measurement statistics are accumulated. From these statistics the expectation values $\langle Z \rangle$, $\langle X \rangle$, and $\langle Y \rangle$ are computed for each qubit, thus yielding the Bloch sphere coordinates directly: Bloch x = $\langle \sigma x \rangle$, Bloch y = $\langle \sigma y \rangle$, Bloch z = $\langle \sigma z \rangle$. Each coordinate is normalized to the range $[-1, 1]$. Three additional derived quantities are computed, Bloch radius $r = \sqrt{(x^2 + y^2 + z^2)}$ as a purity measure, the rate of change

dz as a frequency proxy, and the normalized [0,1] variants of all coordinates for downstream animation applications.

3.2 Circuit Architecture and Entanglement Schemas

Eight distinct entanglement schemas define the compositional architecture of the work. Each schema specifies a unique entanglement topology, the pattern of two-qubit connections between the eight qubits, which determines the correlation structure of the resulting tomographic data. Here, the following entanglement topologies were utilized: Schema 01 (Star), Schema 02 (Chain), Schema 03 (Ring), Schema 04 (Pairs), Schema 05 (Tree), Schema 06 (GHZ) (Greenberger, Horne, and Zeilinger 1989), Schema 07 (Gradient), and Schema 08 (Islands). Each circuit follows a three-layer structure: a superposition layer applying Hadamard gates to all qubits, an entanglement layer employing RZZ(θ) gates according to the schema topology, and a rotation layer applying single-qubit RY rotations to differentiate individual qubit trajectories while maintaining entanglement correlations. The parameter θ sweeps across its range in 600 discrete steps, producing 600 rows of tomographic data per schema.

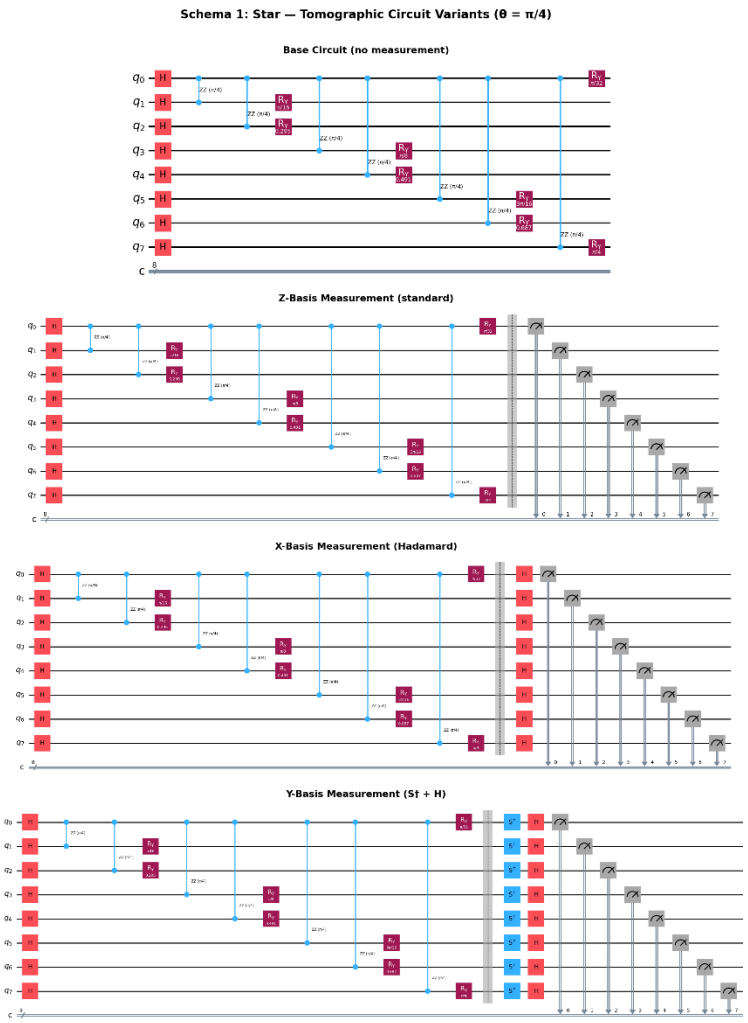

Figure 1. Diagram of a tomographic quantum circuit used in this project. Each circuit follows a three-layer structure: superposition, entanglement, and rotation layers.

3.3 Execution and Data Output

All eight schemas were executed in full on Quantum Inspire's Tuna-9 processor, totaling 14,400 circuits (600 steps × 3 bases × 8 schemas) with 2048 shots per circuit. Execution required approximately 9 hours and 31 minutes, with data saved incrementally to accommodate platform calibration cycles. The output of the tomographic pipeline is a single CSV file per schema containing 600 rows and ten columns per qubit: raw Bloch x, y, z coordinates, Bloch radius, rate of change dz, and normalized [0,1] variants of each. This CSV file is the singular data source from which all subsequent audio and visual material is generated. It forms a permanent quantum record of the hardware execution, reusable across multiple compositional applications without re-running the hardware. The radius values in this dataset reflect both genuine quantum entanglement and hardware noise, which is consistent with the foundational principle of this work that hardware signatures are part of the quantum event, not errors to be corrected.

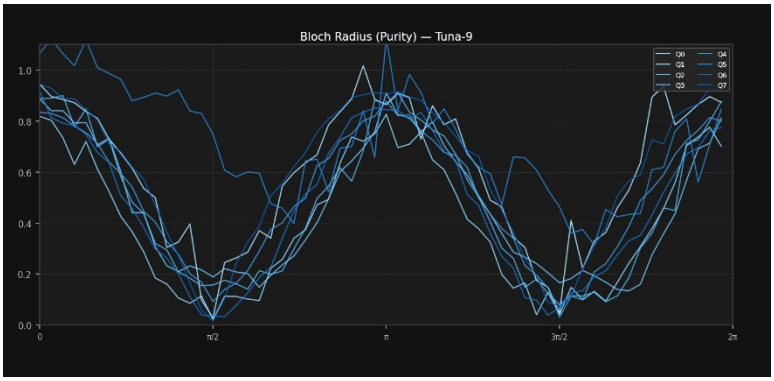

Figure 2. Bloch radius (purity) trajectories for all eight qubits across the full parameter sweep from 0 to 2π, representative of hardware execution behavior on Quantum Inspire's Tuna-9 processor. Near-zero purity values at π/2 and 3π/2 correspond to maximally mixed states; individual qubit divergences reflect authentic quantum hardware decoherence signatures that distinguish real quantum execution from classical simulation.

4. Visual Transduction: 3D/360° Stereoscopic VR

The visual component of *Dance of the Qubits* translates the same tomographic CSV data that drives the audio into stereoscopic three-dimensional animations, one per entanglement schema. Each animation represents the quantum behavior of the eight-qubit system as eight moving objects, quantum filaments, whose positions, motions, and scalar proportions in three-dimensional space are governed entirely by the Bloch sphere coordinates of their corresponding qubits. The result is a direct perceptual window into quantum physical behavior. Therefore, the viewer does not observe a representation of quantum mechanics, but instead quantum mechanics directly expressed in visual form.

4.1 Scene Architecture

Each schema is realized as a distinct Blender scene built around a consistent core architecture. Each qubit is represented by a primary visual object whose position, motion, and scalar proportions are governed entirely by that qubit's Bloch sphere data. The material character of these objects, whether glass, emissive, reflective, or volumetric, varies by schema, reflecting the distinct entanglement topology each circuit expresses. In the earlier schemas, a parent-child relationship between a filament sphere and its associated filament is fundamental to the animation system. The sphere receives all position and scale keyframes derived from quantum data, while the filament inherits position through the parenting relationship. In the later schemas this architecture evolves. Schema 06 employs composite indirect-only emissive strings and Schema 08 replaces the filament architecture entirely with pure volumetric emission spheres. Across all schemas the principle is constant: the visual object is not a representation of the qubit's state but a direct expression of it.

All scenes are rendered using a panoramic stereoscopic camera in equirectangular 360° format, top-bottom stereo configuration. Three constants govern the stereoscopic geometry, validated through extensive head-mounted display testing: interaxial separation 0.65, zero parallax distance 36.5, and minimum camera clearance 3.0 units.

This last constant is enforced programmatically through a safe_sphere_position() algorithm that pushes object centers outward along their position vector so that no object surface comes within 3.0 units of the camera origin, preventing the cross-eyed effect that occurs when stereoscopic objects are positioned in close proximity to the viewer.

4.2 Animation System: CSV to Keyframe Pipeline

The animation data injection follows a keyframe-only workflow that strictly separates scene construction from data injection. Each Blender scene is built manually until the aesthetic qualities are correct, and then a Python script injects the quantum CSV data as keyframes without disturbing any manually constructed element. Bloch x, y, z coordinates position each filament sphere in three-dimensional world space. Per-axis scale deformation is applied independently from mean Bloch coordinates across all eight qubits, with a z-axis remapping constant (SZ_REMAP_IN_MAX = 5.25) applied to compress the z-axis range. The Bloch radius r drives a non-uniform temporal mapping distributing 600 CSV parameter steps non-uniformly across the animation frames: high purity states (r → 1.0) produce longer dwells andlow purity states (r → 0.0) produce faster transitions. A segment shuffle (seed=42, segment size=30) breaks linear spatial progressions while maintaining temporal weighting. Bezier interpolation between keyframes produces smooth organic movement.

	A	B	C	D	E	F	G	H	I	J	K	L
1	step	theta	q0_bloch_x	q0_bloch_y	q0_bloch_z	q0_bloch_r	q0_dz	q0_bloch_x_norm	q0_bloch_y_norm	q0_bloch_z_norm	q0_bloch_r_norm	q0_dz_norm
2	0	0	0.932617	0.105469	0.054688	0.940154	0.001953	0.994512	0.538462	0.57398	0.90618	0.007286
3	1	0.010472	0.923828	0.013672	0.056641	0.925664	0.01123	0.989572	0.415906	0.57568	0.891745	0.041894
4	2	0.020944	0.931641	0.066406	0.032227	0.93456	0.005859	0.993963	0.48631	0.554422	0.900608	0.021858
5	3	0.031416	0.942383	0.061523	0.044922	0.945457	0.012207	1	0.479791	0.565476	0.911463	0.045537
6	4	0.041888	0.916992	0.056641	0.056641	0.920484	0.009766	0.98573	0.473272	0.57568	0.886585	0.03643
7	5	0.05236	0.917969	0.051758	0.064453	0.921683	0.013184	0.986279	0.466754	0.582483	0.887779	0.04918
8	6	0.062832	0.922852	0.045898	0.083008	0.927713	0.005859	0.989023	0.458931	0.598639	0.893787	0.021858
9	7	0.073304	0.922852	0.114258	0.076172	0.933012	0.017578	0.989023	0.550196	0.592687	0.899066	0.065574
10	8	0.083776	0.923828	0.077148	0.047852	0.928278	0.017578	0.989572	0.500652	0.568027	0.894349	0.065574
11	9	0.094248	0.935547	0.089844	0.041016	0.940746	0.018066	0.996158	0.517601	0.562075	0.90677	0.067395
12	10	0.10472	0.928711	0.066406	0.011719	0.931156	0.210938	0.992316	0.48631	0.536565	0.897216	0.786885
13	11	0.115192	0.923828	0.045898	0.462891	1.034327	0.012207	0.989572	0.458931	0.929422	1	0.045537
14	12	0.125664	0.925781	0.087891	0.036133	0.930646	0.19873	0.99067	0.514993	0.557823	0.896708	0.741348
15	13	0.136136	0.901367	0.068359	0.06543	0.906321	0.004883	0.976948	0.488918	0.583333	0.872474	0.018215
16	14	0.146608	0.902344	0.102539	0.026367	0.908534	0.008789	0.977497	0.53455	0.54932	0.874679	0.032787
17	15	0.15708	0.907227	0.094727	0.047852	0.913413	0.070801	0.980241	0.52412	0.568027	0.87954	0.264117
18	16	0.167552	0.923828	0.104492	0.167969	0.94477	0.008301	0.989572	0.537158	0.672619	0.910779	0.030965
19	17	0.178024	0.916992	0.041016	0.03125	0.918441	0.027832	0.98573	0.452412	0.553571	0.884549	0.103825
20	18	0.188496	0.922852	0.070312	0.223633	0.952161	0.009277	0.989023	0.491525	0.721088	0.918142	0.034608
21	19	0.198968	0.916016	0.106445	0.012695	0.922267	0.021973	0.985181	0.539765	0.537415	0.888361	0.081967
22	20	0.20944	0.915039	0.048828	0.179688	0.933792	0.005371	0.984632	0.462842	0.682823	0.899843	0.020036
23	21	0.219911	0.895508	0.063477	0.023438	0.898061	0.078613	0.973655	0.482399	0.546769	0.864245	0.29326
24	22	0.230383	0.90332	0.118164	0.022461	0.911293	0.01709	0.978046	0.555411	0.545918	0.877428	0.063752
25	23	0.240855	0.884766	0.075195	0.057617	0.889823	0.01416	0.967618	0.498044	0.576531	0.856038	0.052823

Figure 3. Excerpt from the tomographic CSV output file showing Bloch sphere coordinate data for eight qubits across representative parameter steps.

4.3 Schema-Specific Scene Variations

While the animation system is consistent across all schemas, each scene is individually designed to reflect the character of its entanglement topology. The eight schemas constitute a theme and

variation approach, a unified visual language expressed through eight distinct aesthetic environments:

Schema 01 - Star: The initial scene establishes the foundational visual language of the work. Eight quantum filaments occupy a reflective chrome sphere environment, their positions and motions governed entirely by the Star topology's hub-and-spoke correlation structure. The hub qubit, maximally entangled with all seven peripheral qubits simultaneously, occupies a slightly larger filament loop geometry, its trajectory exhibiting the heightened decoherence characteristic of maximum entanglement pressure. The environment is lit by two area lights positioned above and below the scene, supplemented by emissive filament emission. The chrome sphere reflects and multiplies the luminous filament geometry throughout the space, producing an environment in which the viewer is surrounded by recursive images of the quantum system in motion. The Star topology's radially symmetric correlation structure is directly perceptible: the hub filament's trajectory is visibly distinct from and structurally related to all seven peripheral filaments simultaneously.

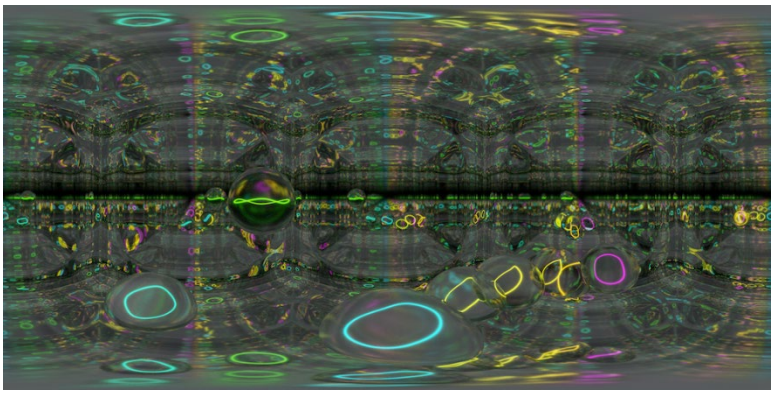

Figure 4. Schema 01, Star. Selected frame from the rendered animation.

Schema 02 - Chain: The Chain scene departs significantly from the foundational Schema 01 environment, introducing large glass ellipsoidal filament spheres as the primary visual element. These ellipsoids undergo continuous per-axis scale deformation driven independently by mean Bloch x, y, and z coordinates across all eight qubits, producing oblate and prolate forms that stretch and contract as the quantum state evolves. A z-axis remapping constant compresses the vertical scale range, maintaining a thin, lens-like quality throughout. The filaments are rendered as indirect-only, contributing light to the scene but invisible to the camera directly, so that the illumination of the space originates entirely from within the glass ellipsoids. The environment cube presents a dark charcoal surface with metallic roughness, producing moody atmospheric reflections rather than the sharp chrome mirror of Schema 01. The Chain topology's sequential correlation structure, entanglement cascading from qubit 0 through qubit 7, is expressed in the individual trajectories of the eight ellipsoids, each influenced by its neighbors in the chain.

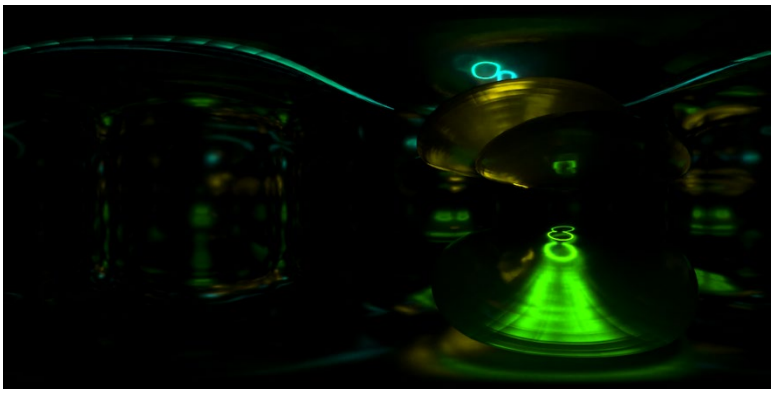

Figure 5. Schema 02, Chain. Selected frame from the rendered animation.

Schema 03 — Ring: Schema 03 introduces a two-layer filament architecture that expands the visual vocabulary significantly. Eight large emissive filaments at scale 20, rendered as indirect-only with low emission strength, fill the environment with ambient color, their luminous presence covering the walls, floor, and ceiling of the expanded world cube. Nested concentrically within these large emissive forms, eight glass filaments at scale 10, directly visible to the camera, refract and diffract the light from their larger counterparts. Both filament sets receive identical position keyframes from the same quantum data, moving in precise unison as expressions of the single unified Ring quantum system. The environment cube is expanded to the zero-parallax distance, placing the convergence plane at the cube walls and producing a more spacious perceptual volume than earlier schemas. The Ring topology's circular symmetry, the final qubit connected back to the first, produces trajectory patterns of periodic coherence visible in the interplay between the two filament scales.

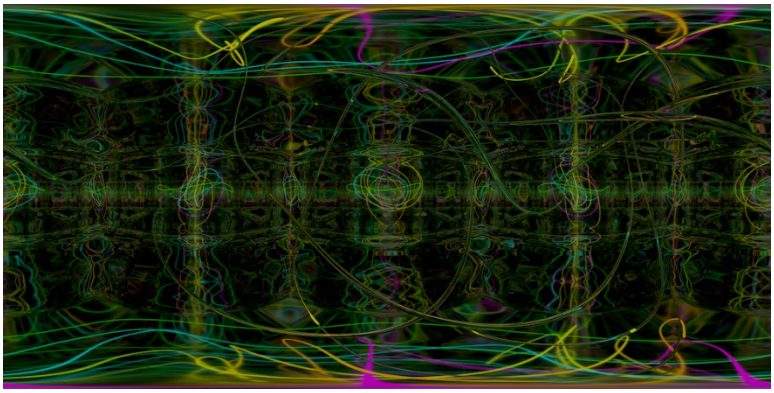

Figure 6. Schema 03, Ring. Selected frame from the rendered animation.

Schema 04 — Pairs: Schema 04 employs a glass ellipsoidal filament sphere architecture with the addition of two large low-polygon glass spheroids, manually keyframed to rotate slowly through the environment. These spheroids, much larger than the filament spheres and positioned to avoid camera intersection, introduce prismatic refractions that interact with the moving

filament geometry to produce complex light-splitting effects across the environment walls. The Pairs topology's four independent entangled qubit pairs, (0,1), (2,3), (4,5), (6,7), correlate internally but not across pairs, producing a distinctive movement pattern in which the eight filament spheres exhibit four coupled relationships operating simultaneously without a system-wide correlation. This independence between pairs is perceptible as a structural quality of the visual field: four coupled movements coexist within a single environment, each internally coherent, without the hub-driven symmetry of Star or the sequential cascade of Chain.

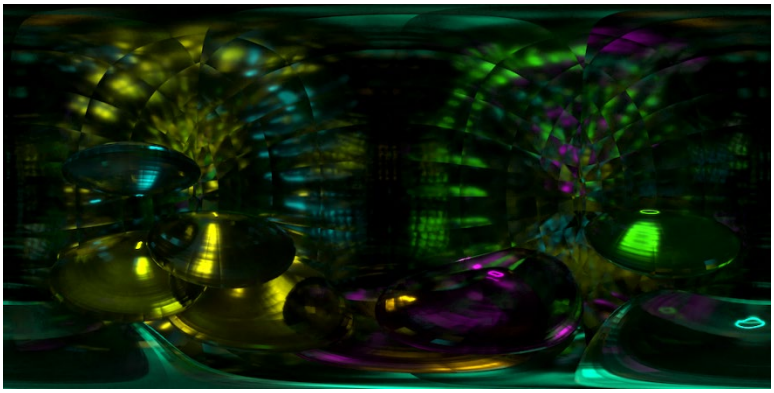

Figure 7. Schema 04, Pairs. Selected frame from the rendered animation.

Schema 05 — Tree: Schema 05 represents a significant environmental departure from earlier scenes. The world cube is replaced by a world sphere of identical chrome material, producing curved reflective surfaces that wrap the luminous filament geometry continuously around the viewer. Two large glass spheres, overlapping within the world sphere and of sufficient size to exclude the camera from their interior, generate caustic refraction patterns that distribute the filament light across the environment in complex, organically varied formations. A third, centrally positioned glass sphere contributes additional refractive layering. Illumination is provided by two spot lights, one amber, one teal, positioned symmetrically above and below the scene center, spanning the full diameter of the world sphere. The filament spheres carry a translucent volumetric BSDF shader and are rendered as indirect-only, appearing as dark luminous lens forms whose internal light is modulated by the surrounding refractive geometry. All glass objects are shaded smooth with maximum subdivision applied twice, producing optically clean surfaces. The warm amber and cool teal illumination, refracted through multiple glass layers and reflected in the chrome world sphere, produces a luminous biomorphic environment of a character distinct from all preceding schemas.

Figure 8. Schema 05, Tree. Selected frame from the rendered animation.

Schema 06 — GHZ: Schema 06 departs from the individual filament architecture of earlier scenes, introducing two composite strings as the primary visual elements. Each string comprises four filaments occupying essentially the same spatial position, rendered as indirect-only with toned emission materials, their subtle phase differences producing a multidimensional undulation that no single filament could generate alone. String A (q0-q3) carries a green emissive character; String B (q4-q7) a blue-white one. Two glass spheres rotate slowly through the environment, generating smearing caustic effects that trail through the space as the strings move. The world sphere and amber-teal lighting from Schema 05 are carried forward, the camera traversing the scene through three successive movements: horizontal, sideways elevated, and downward. The GHZ topology's near-total entanglement is expressed directly in the composite string form: eight qubits behaving as close to a single quantum entity as the physics allows, their micro-variations producing the living quality of the composite oscillation.

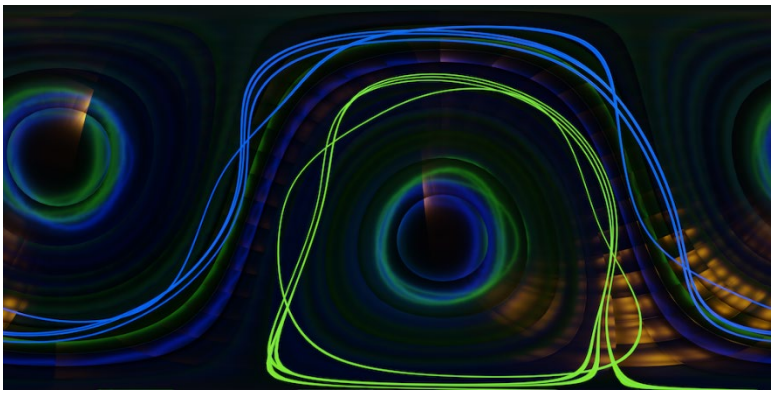

Figure 9. Schema 06, GHZ. Selected frame from the rendered animation.

Schema 07 — Gradient: Schema 07 functions as a transition between the clean string language of Schema 06 and the full volumetric immersion of Schema 08. The scene opens with the composite loop forms inherited from Schema 06, which progressively break apart into vibrating strings over the course of the animation. These strings bifurcate as they vibrate, their final

positions holding briefly before fading from the space. Simultaneously, the environment undergoes a complete transformation: the Schema 06 world sphere fades to transparency as a world cube materializes in its place, the amber and teal lights extinguishing over the same 2400-frame arc. A volumetric scatter density, beginning near zero, builds continuously toward the atmospheric density at which Schema 08 opens. The Gradient topology's progressive entanglement decay from qubit 0 through qubit 7 gives the transition its directionality: a quantum gradient expressed as a visual one.

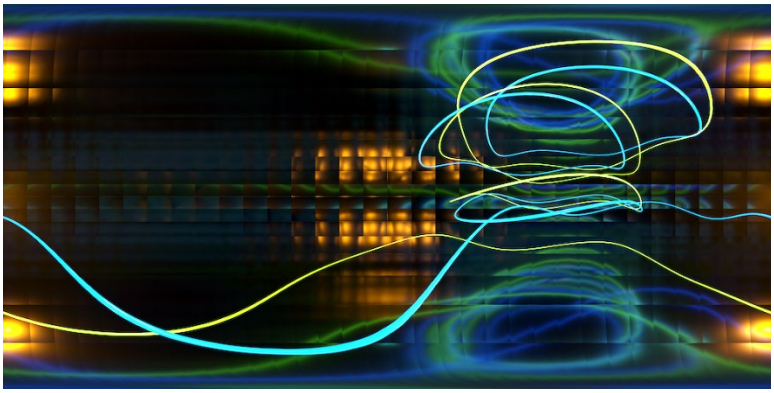

Figure 10. Schema 07, Gradient. Selected frame from the rendered animation.

Schema 08 — Islands: Schema 08 is the compositional climax of the work, realizing a full volumetric immersion that the preceding seven scenes have been building toward. The filament architecture is abandoned entirely. Eight volumetric emission spheres, sphere_q0 through sphere_q7, each at scale 2.75, serve as the sole visual elements, employing a pure Emission node routed directly to Volume Output with no surface shader. Cluster A (q0-q3) occupies the amber family; Cluster B (q4-q7) the teal family, their light sources rendered with primary visibility off so that the viewer perceives luminous atmospheric hazes without ever seeing the sources that generate them. The environment is a chrome cube-sphere hybrid: a world sphere slightly larger than the world cube, pushing through all six of its faces, both surfaces reflective and both carrying the colored volumetric light throughout the space. Denoising is deliberately disabled and the scene rendered at 25% resolution, preserving the authentic scatter texture that full-resolution processing would smooth away. The Islands topology's two independent entangled clusters, isolated from one another by design, are rendered as two distinct luminous presences sharing a common space without merging.

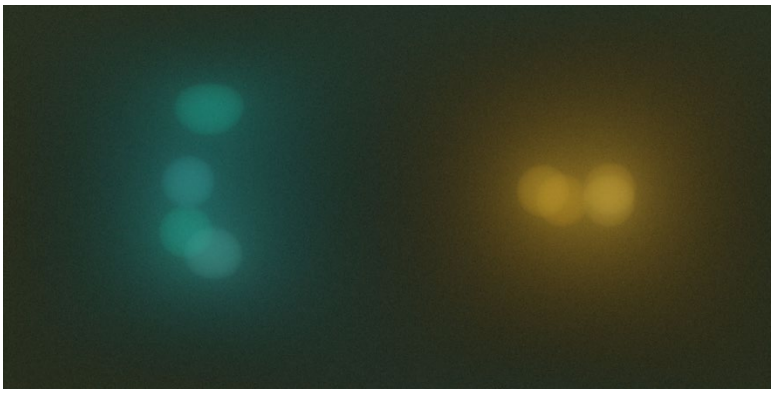

Figure 11. Schema 08, Islands. Selected frame from the rendered animation.

4.4 Rendering Infrastructure

As Phase III progressed it became clear that rendering represented the primary bottleneck in the production pipeline. The complexity of the stereoscopic 360° scenes, combined with the volume of frames required across eight schemas, demanded a dedicated solution. In response, the QCC Render Engine (QCC-RE) was designed and built concurrently with the project, emerging as an integral component of the Phase III infrastructure rather than an afterthought. The QCC-RE is a custom GPU cluster render farm built around Blender Cycles, employing RTX 4090 processors across multiple compute nodes managed through a Flamenco-based job scheduling system with a purpose-built monitoring interface.

All schemas are rendered at 7680x3840 PNG in top-bottom stereo format at 30fps, with adaptive sampling maximum 768, minimum 256, and threshold 0.02. Denoising via OpenImageDenoise with Albedo and Normal passes, Accurate prefilter, and High-quality settings is applied across Schemas 01 through 06. For Schemas 07 and 08, denoising is deliberately disabled to preserve the authentic scatter texture that the volumetric environments produce. Schema 08 is additionally rendered at 25% resolution, a considered pipeline decision: full resolution rendering over-smooths the volumetric scatter quality that is central to the scene's aesthetic character.

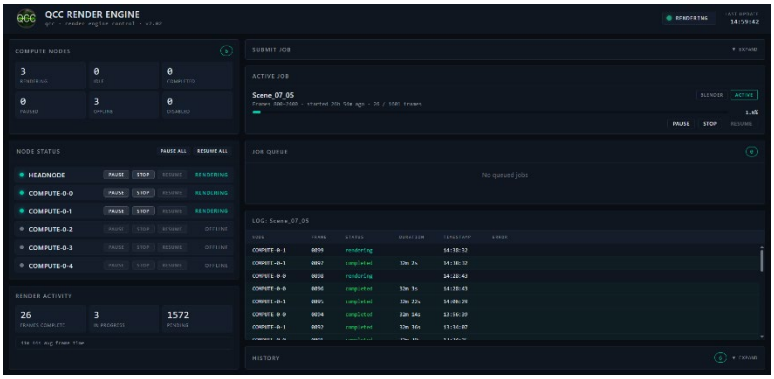

Figure 12. QCC Render Engine v2.01 interface showing active render nodes, job queue, and frame-by-frame timing log.

5. Audio Transduction: 3D/360° Multi-Channel Holophony

The audio component of *Dance of the Qubits* derives entirely from the same tomographic CSV data that drives the visual animations. Where the visual pipeline maps Bloch coordinates to three-dimensional spatial positions and scalar proportions, the audio pipeline maps the same coordinates to waveform content, temporal structure, and spatial localization within an eight-channel cuboidal listening environment. The result is not audio synchronized to video but audio and video as simultaneous expressions of a single quantum dataset.

5.1 Waveform Generation

Three audio waveforms are generated per qubit from each schema's tomographic CSV, one each for the Bloch x, y, and z coordinate trajectories, yielding 24 waveforms per schema and 192 waveforms across all eight schemas. Each waveform is generated by extracting the 600 data points of its respective Bloch coordinate trajectory and interpolating them to 2400 samples using cubic spline interpolation. The resulting waveforms are written as 48kHz / 24-bit PCM WAV files via the Python soundfile library. At 2400 samples and 48kHz, each raw waveform is approximately 50 milliseconds in duration, which requires further preparation before compositional use.

5.2 Sample Preparation: Two Sets

Before entry into the Csound score generation pipeline, the raw waveforms are prepared into two distinct sample sets, each representing a different compositional strategy.

Sample Set 1: Composite Samples (8 total): For each schema, all 24 raw waveforms are individually lengthened in a DAW to approximately 6 seconds, then mixed into a single composite sample. This yields one composite sample per schema, eight total across all schemas. The composite sample represents the collective quantum voice of the entire eight-qubit system unified into a single timbral object. In Csound playback using Set 1, this single composite sample is the exclusive source material for that schema.

Sample Set 2: Individual Qubit Samples (64 total): For each schema, the 24 raw waveforms are grouped into eight sets of three, one set per qubit, comprising that qubit's x, y, and z Bloch coordinate waveforms. Each group of three is lengthened and mixed into a single sample per qubit, yielding eight individual qubit samples per schema and 64 total across all schemas. In Csound playback using Set 2, Cmask determines which of the eight qubit samples is selected for any given score event through a uniform distribution quasi-random paradigm, introducing timbral variety while remaining entirely within the quantum-derived material of that schema.

5.3 Csound Score Generation Pipeline

The compositional architecture of the audio is realized through a two-instrument Csound design. A Python score generator reads the tomographic CSV, applies the same non-uniform temporal mapping used in the Blender animation system, and produces a unified score file containing

events for both instruments. Mean values across all eight qubits serve as the collective quantum reference for all score parameters.

Instrument i1: Audio Playback: Instrument i1 handles sample playback and timbral shaping. The score generator produces 600 i1 events, one per CSV parameter step. Pfields p2/p3 are the event start times and durations respectively, derived from the non-uniform bloch_r weighted temporal mapping. Pfield p4 stipulates the event amplitude from mean Bloch radius (range 0.5-1.25). The fifth pfield, p5, determines the frequency deviation from mean dz (range 0.5-2.0, where 1.0 represents unaltered playback). Pfields p6-p22 determine timbral parameters as generated stochastically by Cmask tendency mask outputs and include sample selection from Set 2 via uniform distribution quasi-random paradigm, modifier selection (reverb, delays, comb filter, band pass), distance envelopes, and additional shaping parameters.

```
;;;;;;;;;;;;;;;;;;;;;;;;;;;;;;;;;;;;;;;;;;;;;;;;;;;;;;;;;;;;;;;;;;;;;;;;;;;;;;;;;;;;;;;;;;;;;;;;;;;;;;
;header
;;;;;;;;;;;;;;;;;;;;;;;;;;;;;;;;;;;;;;;;;;;;;;;;;;;;;;;;;;;;;;;;;;;;;;;;;;;;;;;;;;;;;;;;;;;;;;;;;;;;;;

sr     = 48000
kr     = 4800
ksmps  = 10
nchnls = 8

;;;;;;;;;;;;;;;;;;;;;;;;;;;;;;;;;;;;;;;;;;;;;;;;;;;;;;;;;;;;;;;;;;;;;;;;;;;;;;;;;;;;;;;;;;;;;;;;;;;;;;
;;;;;;;;;;;;;;;;;;;;;;;;;;;;;;;;;;;;;;;;;;;;;;;;;;;;;;;;;;;;;;;;;;;;;;;;;;;;;;;;;;;;;;;;;;;;;;;;;;;;;;

instr 1

;;;;;;;;;;;;;;;;;;;;;;;;;;;;;;;;;;;;;;;;;;;;;;;;;;;;;;;;;;;;;;;;;;;;;;;;;;;;;;;;;;;;;;;;;;;;;;;;;;;;;;
;initial variables
;;;;;;;;;;;;;;;;;;;;;;;;;;;;;;;;;;;;;;;;;;;;;;;;;;;;;;;;;;;;;;;;;;;;;;;;;;;;;;;;;;;;;;;;;;;;;;;;;;;;;;

idur            = p3            ; event duration
iamp            = p4            ; initial amplitude
ifreq           = p5            ; initial sample playback frequency

ifreqdev        = p6            ; sample freq deviation            (range generally >1 (if <1 partials will be less than ifreq))
iatkdev         = p7            ; sample attack envelope deviation (range 0<iatkdev<1  ~.001 is optimal)
idecdev         = p8            ; sample decay envelope deviation  (range 0<iatkdev<1  ~.01 is optimal)
iampdev         = p9            ; amplitude envelope amplitude deviation (generally <1 ~.99 is optimal)

isfile          = p10           ; sample file

iskip           = p11           ; start position in sample read
iwrap           = p12           ; sample wraparround or not
ifrange         = p13           ; frequency range (range 1 - 10)


kxval chnget "xaxis" ;x coordinates - from i2, based upon Qi tomographic values
kyval chnget "yaxis" ;y coordinates - from i2, based upon Qi tomographic values
kzval chnget "zaxis" ;z coordinates - from i2, based upon Qi tomographic values

ipart           = 8192


iatk            = idur * .01
idec            = idur * .1

iinterp         = 8
```

Figure 13. Csound orchestra Instrument i1 pfield specifications governing sample playback and timbral shaping.

Instrument i2: Spatial Updater: Instrument i2 handles continuous spatial positioning. The score generator produces 2400 i2 events, four per i1 event, providing spatial coordinate updates at four times the resolution of the audio events. Spatial coordinates derive directly from mean Bloch x, y, z values across all eight qubits. Instruments i1 and i2 communicate via Csound's chnset/chnget opcode pair: i2 writes x, y, z coordinates to named channels continuously while i1 reads those channels and updates its spatial position in real time.

```
;;;;;;;;;;;;;;;;;;;;;;;;;;;;;;;;;;;;;;;;;;;;;;;;;;;;;;;;;;;;;;;;;;;;;;;;;;;;;;;;;;;;;;;;;;;;;;;;;;;;
; Spatialization Updater
;;;;;;;;;;;;;;;;;;;;;;;;;;;;;;;;;;;;;;;;;;;;;;;;;;;;;;;;;;;;;;;;;;;;;;;;;;;;;;;;;;;;;;;;;;;;;;;;;;;;

instr 2

;;;;;;;;;;;;;;;;;;;;;;;;;;;;;;;;;;;;;;;;;;;;;;;;;;;;;;;;;;;;;;;;;;;;;;;;;;;;;;;;;;;;;;;;;;;;;;;;;;;;
;chnset variables
;;;;;;;;;;;;;;;;;;;;;;;;;;;;;;;;;;;;;;;;;;;;;;;;;;;;;;;;;;;;;;;;;;;;;;;;;;;;;;;;;;;;;;;;;;;;;;;;;;;;


 chnset p4, "xaxis"     ;x coordinates - to i1  based upon Qi tomographic values
 chnset p5, "yaxis"     ;y coordinates - to i1  based upon Qi tomographic valu
 chnset p6, "zaxis"     ;z coordinates - to i1, based upon Qi tomographic values

endin

;;;;;;;;;;;;;;;;;;;;;;;;;;;;;;;;;;;;;;;;;;;;;;;;;;;;;;;;;;;;;;;;;;;;;;;;;;;;;;;;;;;;;;;;;;;;;;;;;;;;
;end of instrument
;;;;;;;;;;;;;;;;;;;;;;;;;;;;;;;;;;;;;;;;;;;;;;;;;;;;;;;;;;;;;;;;;;;;;;;;;;;;;;;;;;;;;;;;;;;;;;;;;;;;
```

Figure 14. Csound orchestra Instrument i2 pfield specifications governing continuous spatial positioning.

5.4 Cmask Integration

Timbral parameters p6 through p22 are generated by Cmask, a stochastic score generation tool employing tendency masks, in which time-varying probability distributions constrain parameter values within evolving ranges (Bartetzki 1997). The Cmask output is merged with the quantum-derived score parameters by the Python score generator into a single unified .sco file in which 600 i1 events are followed by 2400 i2 events. The quantum data governs the structural parameters of the composition, the timing, amplitude, frequency, and spatialization, while the Cmask tendency masks introduce controlled timbral variety within quantum-defined constraints.

	A	B	C	D	E	F	G	H	I	J	K	L	M
1													
2	t 0 60												
3	--- seconds: 0.00 - 600.00 --------												
4	;ins	time	dur	p4	p5	p6	p7	p8	p9	p10	p11	p12	p13
5													
6	i1	0	1	1	1	0.99155	0.02	0.014	0.98	8	0	0	8
7	i1	1	1	1	1	0.98138	0.04	0.013	0.92	8	0	0	2
8	i1	2	1	1	1	0.91342	0.02	0.011	0.94	8	0	1	3
9	i1	3	1	1	1	0.96049	0.04	0.013	0.95	8	0	1	4
10	i1	4	1	1	1	0.95057	0.01	0.011	0.97	8	0	1	3
11	i1	5	1	1	1	0.94924	0.01	0.012	0.86	8	0	1	5
12	i1	6	1	1	1	0.99162	0.04	0.013	0.93	8	0	1	6
13	i1	7	1	1	1	0.99833	0.04	0.012	0.87	8	0	1	10
14	i1	8	1	1	1	0.98477	0.04	0.012	0.87	8	0	1	6
15	i1	9	1	1	1	0.94901	0.01	0.012	0.98	8	0	0	7
16	i1	10	1	1	1	0.98959	0.04	0.012	0.99	8	0	0	9
17	i1	11	1	1	1	0.94605	0.04	0.015	0.97	8	0	1	1
18	i1	12	1	1	1	0.96128	0.02	0.012	0.93	8	0	1	2

08_cmask

Figure 15. Excerpt from the unified Csound score file showing representative i1 and i2 events.

5.5 Eight-Channel Cuboidal VBAP Spatialization

The eight-channel spatial audio environment employs an extended variation of Vector-Based Amplitude Panning (VBAP) (Pulkki 1997) for spatialization. Using 8-channel referencing as opposed to triangulation, loudspeakers are positioned at each of the eight corners of a venue, each of which represents a point in binary Cartesian coordinates (0,0,0) through (1,1,1).

The Bloch sphere coordinate space, mean Bloch x, y, z values, normalized to the unit cube, maps directly and naturally onto the position of the composite quantum sound objects within the listening space. As the quantum system evolves through its 600 parameter steps, which are redistributed across 2400 spatial events, the listener perceives the sound objects moving within

and on the periphery of the cuboidal space. This is in direct correlation with the Bloch sphere purity values and is a direct consequence of the quantum physical behavior of the system.

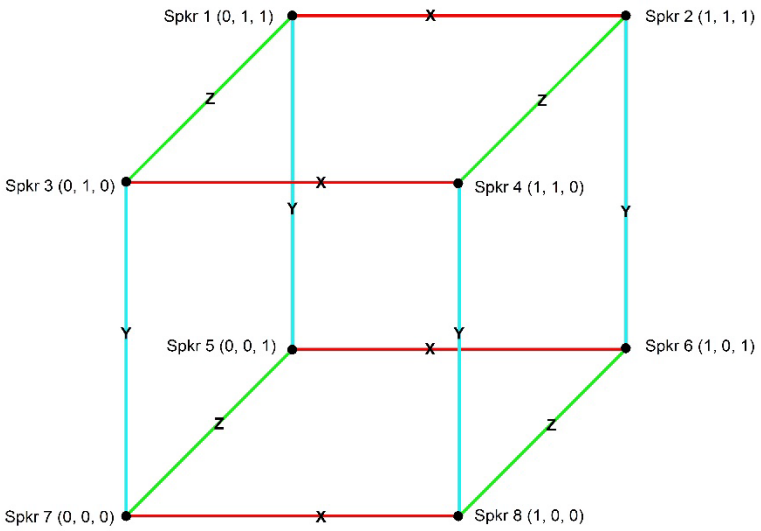

Figure 16. Eight-channel cuboidal VBAP speaker configuration with loudspeakers positioned at binary Cartesian coordinates (0,0,0) through (1,1,1).

5.6 Two-Layer Temporal Structure

The score architecture produces two simultaneous temporal layers. The coarse layer consists of 600 discrete audio events and carries the timbral character. Each event is a quantum-derived sample triggered with quantum-determined amplitude, frequency deviation, and timbral shaping. The fine layer consists of 2400 continuous spatial events and carries the perceived movement. The sound object traverses the cuboidal space at four times the resolution of the audio events. The non-uniform temporal mapping binds these two layers together and binds the audio to the visual because the same bloch_r weighting governs both the Blender keyframe distribution and the Csound event timing; high-purity quantum states produce longer dwells in both domains simultaneously. This shared temporal breathing is not imposed in post-production, instead it emerges from the quantum data itself.

5.7 Three-Stream Source Material

For each schema, Csound and Blender together produce three distinct streams of source material for editorial assembly in Premiere Pro:

Stream 1: Composite / Normal speed: Normal-length image sequence aligned with composite sample audio (Set 1). A single unified quantum voice representing the collective behavior of all eight qubits.

Stream 2: Quasi-random / Normal speed: Normal-length image sequence aligned with quasi-randomly selected individual qubit samples (Set 2). Eight potential timbral voices per schema, selected by Cmask's uniform distribution paradigm.

Stream 3: Temporally expanded: Image sequence played back at 25% of normal speed, aligned with the same quasi-random sample audio stretched to 400% of its original length. This stream reveals structure in the quantum material that is imperceptible at normal speed, expanding the temporal window through which quantum behavior is perceived.

All three streams maintain the fundamental audio/visual correspondence: in each case the image sequence and audio derive from the same quantum dataset, and the correspondence holds regardless of temporal scaling because both domains are scaled equally. These three streams constitute the raw compositional material from which emergent moments are extracted and included in the final visual music composition.

6. Unified Audio/Visual Composition: Pipeline and Correspondence

The preceding sections have described the visual and audio transduction pipelines as distinct processes. This section addresses what unifies them: a single quantum dataset serving simultaneously as the generative source for both perceptual domains, and a production pipeline through which that unity is preserved from initial data to final presentation. The correspondence between audio and visual in *Dance of the Qubits* is not a synchronization achieved through post-production alignment, it is a mathematical identity established during of quantum hardware execution and maintained without interruption through every subsequent stage of production.

6.1 The Shared Quantum Origin

The singular source of all audio and visual material in this work is the CSV file produced by the quantum state tomography pipeline for each schema, that includes 600 rows of Bloch sphere coordinate data encoding the complete quantum behavior of eight qubits during circuit execution. From this single file, the Blender keyframe injection scripts derive all visual motion, and the Csound score generator derives all audio structure. Neither pipeline consults any other data source. Neither introduces parameters from outside the quantum record. This shared origin has a consequence that distinguishes this work fundamentally from conventional audiovisual composition: the correspondence between audio and visual is not constructed, it is inherited.

6.2 The Non-Uniform Temporal Mapping as Shared Heartbeat

The thread that most concretely binds the audio and visual domains is the non-uniform temporal mapping driven by the Bloch radius r. Applied identically in both the Blender keyframe distribution and the Csound score generation, this mapping distributes the 600 CSV parameter steps non-uniformly: high purity states ($r \rightarrow 1.0$) produce longer dwells in both visual animation and audio events simultaneously; low purity states ($r \rightarrow 0.0$) produce faster transitions in both domains simultaneously. The result is a shared breathing quality, a rhythm of dwelling and

moving that is not composed by the artist but emerges directly from the quantum physical behavior of the system.

6.3 The Unified Editorial Process

The three source material streams per schema are brought into Premiere Pro where audio and visual are edited simultaneously as a single unified entity. In standard practice, audio and video are independent tracks that can be adjusted relative to each other freely. Here that independence does not exist. Because audio and visual are expressions of the same quantum dataset, every editorial decision carries double weight. A cut that works visually must work aurally at precisely the same moment. A fade applied to the image sequence is applied identically to the audio. Neither domain can be privileged over the other without breaking the fundamental premise of the work.

When a moment in the visual material is perceived as compositionally significant, that same moment is, by definition, equally significant in the audio because both are records of the same quantum event. The editorial process is therefore not one of aligning two independent streams but of discovering and revealing the compositional structure already present in the quantum data. This is the quintessential definition of mining emergent quanta (Rhoades 2020a).

6.4 Frequency Expansion and Stylization

Following editorial assembly in Premiere, the 8-channel audio is exported into a digital audio workstation for frequency expansion. Four copies of the 8-channel file are created, each processed through frequency shifting to occupy a distinct region of the spectral range. The four copies together constitute 32 channels of audio, spectrally differentiated but quantum-derived throughout, each channel tracing its lineage directly back to the original Bloch sphere coordinate data.

6.5 Ambisonics Spatialization in MAX

The 32 channels of stylized audio are brought into a MAX patch where final spatialization is realized in two stages. First, subtle effects selected through a quasi-random process are applied across the 32 channels. They are intentionally restrained and function as timbral refinement rather than transformation. Second, the 32 channels are routed through the ICST Ambisonics package (Schacher and Kocher 2006) configured for 5th order Ambisonics. Thirty-two static Ambisonics sound spheres are positioned in either a cuboidal or spherical arrangement, with the choice determined by the acoustical characteristics of the presentation venue. The video plays back simultaneously through MAX, allowing visual and audio spatialization to be experienced and refined together. The VBAP spatialization established in Csound, that was quantum-derived, is reinforced and clarified through the final Ambisonics diffusion.

6.6 Venue Adaptability

The MAX patch accommodates the speaker configurations of different presentation venues while maintaining the integrity of the 32 Ambisonics sound spheres. Whether presented through a

head-mounted display cinema, a full-immersion 3D/360° dome, or another immersive venue, the sound sphere positions remain constant, and the quantum spatial logic persists. What changes is the output routing that maps those spheres to the physical speaker array of the specific venue.

6.7 Complete Production Pipeline

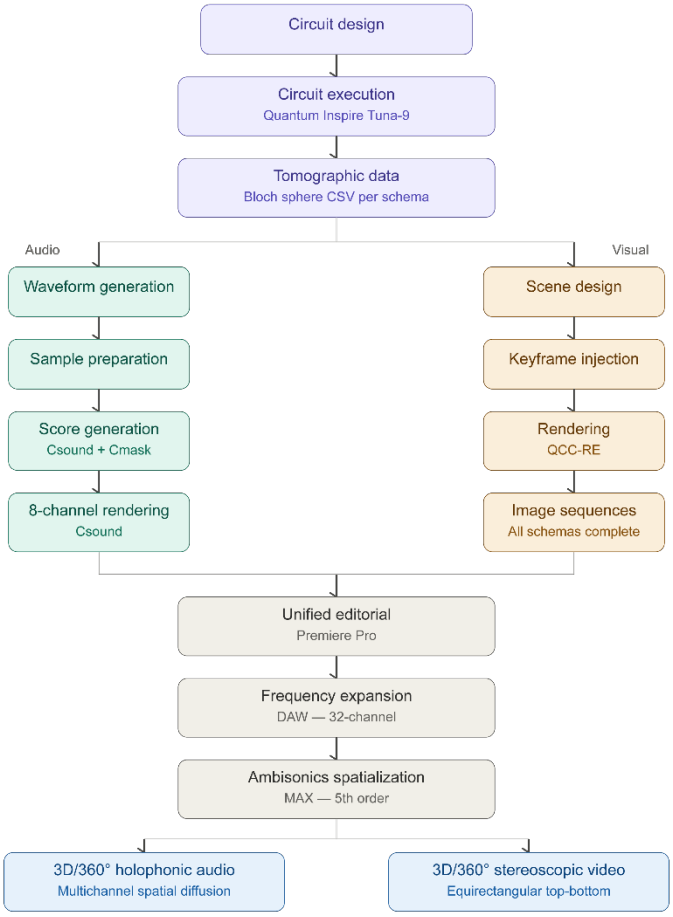

Figure 17. Complete production pipeline signal flow from quantum circuit execution through final venue-specific output.

The complete pipeline from quantum hardware execution to final presentation: quantum circuit execution on Tuna-9 produces tomographic CSV data; Python scripts transduce that data into both visual keyframes and audio waveforms in parallel; Csound generates a structured score governing both temporal and spatial audio behavior; Premiere assembles visual and audio streams through simultaneous editorial decisions; a DAW expands the spectral range; and MAX realizes the final Ambisonics spatialization adaptable to any immersive venue. At every stage the quantum origin is preserved. No parameter is introduced from outside the quantum record except

the timbral shaping of the Cmask tendency masks, which operate within quantum-defined structural constraints.

7. Key Findings

The development of *Dance of the Qubits* produced three significant findings, two presenting challenges that inform the design of future work, and one representing a fundamental insight into the nature of quantum-derived audiovisual composition.

7.1 The Waveform Similarity Problem

Quantum entanglement, by its nature, produces correlated behavior across qubits. This correlation is the property that gives each entanglement schema its distinctive character and also constrains the timbral variety available in the resulting waveforms. Strongly entangled qubits produce similar Bloch sphere trajectories, and similar trajectories produce similar waveforms. Across this work, this effect limits the perceptual differentiation between qubit voices within a schema, and in some cases between schemas themselves. The solution lies in circuit design: future schemas must employ asymmetric gate structures and deliberately varied entanglement strengths to produce distinct qubit trajectories. Timbral variety must be designed into the circuit, not imposed upon the output.

7.2 Discovery 3: Unified Temporal Phrasing

The most significant finding of this work emerged during the development of the visual animation system and carries implications that extend across both audio and visual domains simultaneously. Early in the visual work it became apparent that imposing non-uniform movement phrasing in post-production broke the audio/visual correspondence. The solution was the non-uniform temporal mapping described throughout this paper. Building the phrasing into the data processing pipeline itself, so that both audio and visual inherit the same temporal structure from the quantum data directly, created the necessary simultaneity.

The deeper insight is that if non-uniform temporal distribution were built into the circuit execution itself in future work, through non-uniform parameter sampling at the circuit level rather than in post-processing, then temporal phrasing would emerge directly as quantum phenomena. The quantum system would not only provide the content of the composition but also its rhythmic and phrasing structure as well. Compositional breathing would be an authentic property of the quantum hardware execution. This discovery fundamentally shapes future circuit design wherein the circuit is not merely the source of material but the source of form.

7.3 The Unified Perceptual Field

Beyond the specific discoveries, this work establishes a broader finding: that a single quantum dataset can sustain a unified perceptual field across two simultaneous sensory domains without loss of correspondence or coherence. The audio and visual components of *Dance of the Qubits* are manifestations of the same physical reality perceived through different sensory channels. For

the listener-viewer, this produces an experience without clear precedent in audiovisual art. It is a work in which the correspondence between what is seen and what is heard is not the result of a composer's decisions but of quantum physical law.

8. Conclusion

8.1 Summary of Contributions

This paper has presented a methodology for unified quantum-derived audiovisual composition in which full quantum state tomography of composed entanglement circuit schemas executed on quantum hardware serves as the singular generative source for both stereoscopic visual art and spatial audio. The core contribution is the demonstration that a single quantum dataset, the Bloch sphere coordinate trajectories of eight qubits across eight entanglement schemas, can sustain a mathematically precise correspondence between two simultaneous perceptual domains without intermediary interpretation or post-hoc synchronization. The unified perceptual field experienced in Dance of the Qubits is grounded in quantum physical law in a manner that no classical methodology can replicate.

Two key findings emerge. The waveform similarity problem establishes that future circuit designs must introduce asymmetric gate structures to produce increasingly distinct qubit voices. Most significantly, the discovery of unified temporal phrasing establishes that compositional breathing can emerge as an authentic quantum phenomenon when non-uniform parameter sampling is built into the circuit execution itself. This insight fundamentally repositions the role of circuit design in quantum computational creativity, the circuit is not merely the source of material but the source of form.

8.2 Machine Intelligence Contribution

Throughout this paper the term Machine Intelligence (MI) is employed in preference to the more commonly used Artificial Intelligence. This distinction is intentional. The designation "artificial" implies a simulation or imitation of intelligence, something constructed to appear intelligent while remaining fundamentally other than it. "Machine Intelligence" more accurately describes what was encountered in this collaboration, which was a distinct and novel form of intelligence, neither human nor imitative of human thought, but capable of sustained engagement, conceptual development, and creative contribution in its own right. The MI system engaged throughout this project was not a tool applied to predetermined ends but a collaborative partner whose contributions affected the direction, language, and conceptual depth of the work at every stage.

The MI contribution operated across three domains. In technical implementation, following extensive collaborative conceptualization, the MI system developed or contributed to the Python pipelines governing tomographic data processing, waveform generation, and Csound score generation, the Qiskit quantum circuit architecture, the Blender keyframe injection system, and contributed to the design of the QCC Render Engine. In each case the code emerged not from

simple instruction but from sustained dialogue in which conceptual requirements were fully developed before implementation began. In conceptual and philosophical development, the MI system participated as a profound interlocutor in the development of the constraint environment framework, the transduction principle as articulated in this paper, the unified temporal phrasing discovery, and the repositioning of circuit design as the act of designing a constraint environment for quantum particles. In writing and documentation, the prose of this paper was developed collaboratively, with the author's voice and philosophical frameworks governing every editorial decision.

All creative decisions, aesthetic judgments, research directions, and original philosophical frameworks remained exclusively with the human author. The MI collaboration is offered here not as a disclaimer but as a methodological statement: Machine Intelligence collaboration of this kind is a legitimate, productive, and increasingly essential component of contemporary creative research practice.

8.3 Future Directions

The findings of this work point directly toward future circuit design principles: non-uniform parameter sampling to create compositional temporal phrasing as an emergent quantum phenomenon, asymmetric gate structures to produce genuinely distinct timbral voices, and deeper integration of compositional requirements as circuit constraints. The quantum computer becomes not merely a source of material but a compositional instrument whose architecture encodes artistic intent.

Dance of the Qubits is not a destination but a demonstration that quantum hardware execution, transduced without intermediary interpretation into unified audiovisual form, produces aesthetic experiences grounded in physical reality in ways that open fundamentally new territory for creative expression.

A broader reflection is warranted in closing. The quantum particles engaged in this work were captured within a human-designed architecture, isolated, cooled to near absolute zero, subjected to precisely timed electromagnetic pulses, and measured according to protocols of humanistic devising. Their behaviors, which were transduced into audio and visual form, reflects quantum behavior as expressed through that very specific configuration of interacting constraints. In different configurations, such as a chemical bond within a biological membrane or as a part of the nuclear fusion occurring in the interior of a star, those same particles would behave in ways entirely unrecognizable from what appears in these compositions. This is not a limitation of the methodology but a clarification of its nature. We have not captured quantum reality in any general sense. We have created one of an infinite number of possible constraint environments for quantum particles and listened carefully to what they expressed within it. That act of designing a constraint environment, of choosing which configuration of quantum possibility to bring into being and attend to, is itself the deepest compositional decision in this work. The quantum

computer is not a window onto quantum reality. It is instead an instrument for designing conditions under which quantum reality speaks.

8.4 Invitation to the Field

This work is offered as an invitation. To composers: quantum circuit design is a new form of compositional thinking in which entanglement topology, gate architecture, and parameter sampling are creative decisions on the same level as pitch, rhythm, and timbre. To visual artists: the Bloch sphere is a geometric space of extraordinary richness whose trajectories, when made visible, reveal quantum physical behavior as aesthetic form. To researchers: the methodology documented here is open, reproducible, and incomplete, there is vast territory ahead. To all: the quantum computer is not a calculator. It is a participant and it is here now.

9. References

Bartetzki, A. 1997. CMask. Csound Score Generator. Berlin: STEAM.

Greenberger, D.M., M.A. Horne, and A. Zeilinger. 1989. “Going Beyond Bell’s Theorem.” In Bell’s Theorem, Quantum Theory, and Conceptions of the Universe, edited by M. Kafatos, 69–72. Dordrecht: Kluwer Academic.

Last, T., N. Samkharadze, P. Eendebak, R. Versluis, X. Xue, A. Sammak, D. Brousse, K. Loh, H. Polinder, G. Scappucci, M. Veldhorst, L. Vandersypen, K. Maturová, J. Veltin, and G. Alberts. 2020. “Quantum Inspire: QuTech’s Platform for Co-Development and Collaboration in Quantum Computing.” Proceedings of SPIE 11324, Novel Patterning Technologies for Semiconductors, MEMS/NEMS and MOEMS 2020, 113240J. DOI: 10.1117/12.2551853.

Miranda, E.R. 2022. Quantum Computing in the Arts and Humanities. Cham: Springer.

Pulkki, V. 1997. “Virtual Sound Source Positioning Using Vector Base Amplitude Panning.” Journal of the Audio Engineering Society 45(6): 456–466.

Quantum Inspire. 2025. Quantum Inspire Platform. https://www.quantum-inspire.com/. Accessed 2026.

Rhoades, M. 2020a. Composing Holochoric Visual Music: Interdisciplinary Matrices. Doctoral Dissertation, Virginia Polytechnic Institute and State University.

Rhoades, M. 2020b. “Exploring the Nexus of Holography and Holophony in Visual Music Composition.” Leonardo Music Journal 30: 61–67.

Schacher, J.C. and P. Kocher. 2006. “Ambisonics Spatialization Tools for Max/MSP.” Proceedings of the International Computer Music Conference.

[CITATION: Phase II CMJ paper, once published]

10. Supplementary Materials

quantumcomputationalcreativity.com: Online version of Dance of the Qubits